Overpressure and petroleum generation and accumulation in the Dongying Depression of the Bohaiwan Basin, China

X. XIE[1,2], C. M. BETHKE[2], S. LI[1], X. LIU[1] AND H. ZHENG[3]

[1]*Faculty of Earth Resources, China University of Geosciences, Wuhan, China;* [2]*Department of Geology, University of Illinois at Urbana-Champaign, Urbana, IL, USA;* [3]*Institute of Petroleum Exploration and Development, Shenli Oil Corporation, Dongying, Shandong, China*

ABSTRACT

The occurrence of abnormally high formation pressures in the Dongying Depression of the Bohaiwan Basin, a prolific oil-producing province in China, is controlled by rapid sedimentation and the distribution of centres of active petroleum generation. Abnormally high pressures, demonstrated by drill stem test (DST) and well log data, occur in the third and fourth members (Es3 and Es4) of the Eocene Shahejie Formation. Pressure gradients in these members commonly fall in the range 0.012–0.016 MPa m^{-1}, although gradients as high as 0.018 MPa m^{-1} have been encountered. The zone of strongest overpressuring coincides with the areas in the central basin where the principal lacustrine source rocks, which comprise types I and II kerogen and have a high organic carbon content (>2%, ranging to 7.3%), are actively generating petroleum at the present day. The magnitude of overpressuring is related not only to the burial depth of the source rocks, but to the types of kerogen they contain. In the central basin, the pressure gradient within submember Es32, which contains predominantly type II kerogen, falls in the range 0.013–0.014 MPa m^{-1}. Larger gradients of 0.014–0.016 MPa m^{-1} occur in submember Es33 and member Es4, which contain mixed type I and II kerogen. Numerical modelling indicates that, although overpressures are influenced by hydrocarbon generation, the primary control on overpressure in the basin comes from the effects of sediment compaction disequilibrium. A large number of oil pools have been discovered in the domes and faulted anticlines of the normally pressured strata overlying the overpressured sediments; the results of this study suggest that isolated sandstone reservoirs within the overpressured zone itself offer significant hydrocarbon potential.

Key-words: basin modeling, Bohaiwan Basin, Dongying Depression, overpressure, petroleum accumulation, petroleum generation

INTRODUCTION

Understanding the distribution of overpressure in a sedimentary basin plays an important role in petroleum exploration, drilling and oil field development and production (Fertl *et al.* 1994). The origin of abnormally high formation pressure, however, is not always clear and a number of mechanisms for generating pressures in excess of hydrostatic have been proposed (Fertl *et al.* 1994; Hubbert & Rubey 1959; Hunt 1990; Law & Spencer 1998; Luo & Vasseur 1996). Among these, important mechanisms in extensional basins include disequilibrium sediment loading and compaction and the increase in fluid volume resulting from hydrocarbon generation. The former mechanism has been applied to explain overpressure in young sediments undergoing rapid sedimentation, such as the Gulf Coast Basins (Bethke 1986; Dickinson 1953) and the Yinggehai Basin (Xie *et al.* 1999). The latter mechanism has been invoked in some older basins, such as the Uinta Basin (Bredehoeft *et al.* 1994) and the Delaware Basin (Lee & Williams 2000).
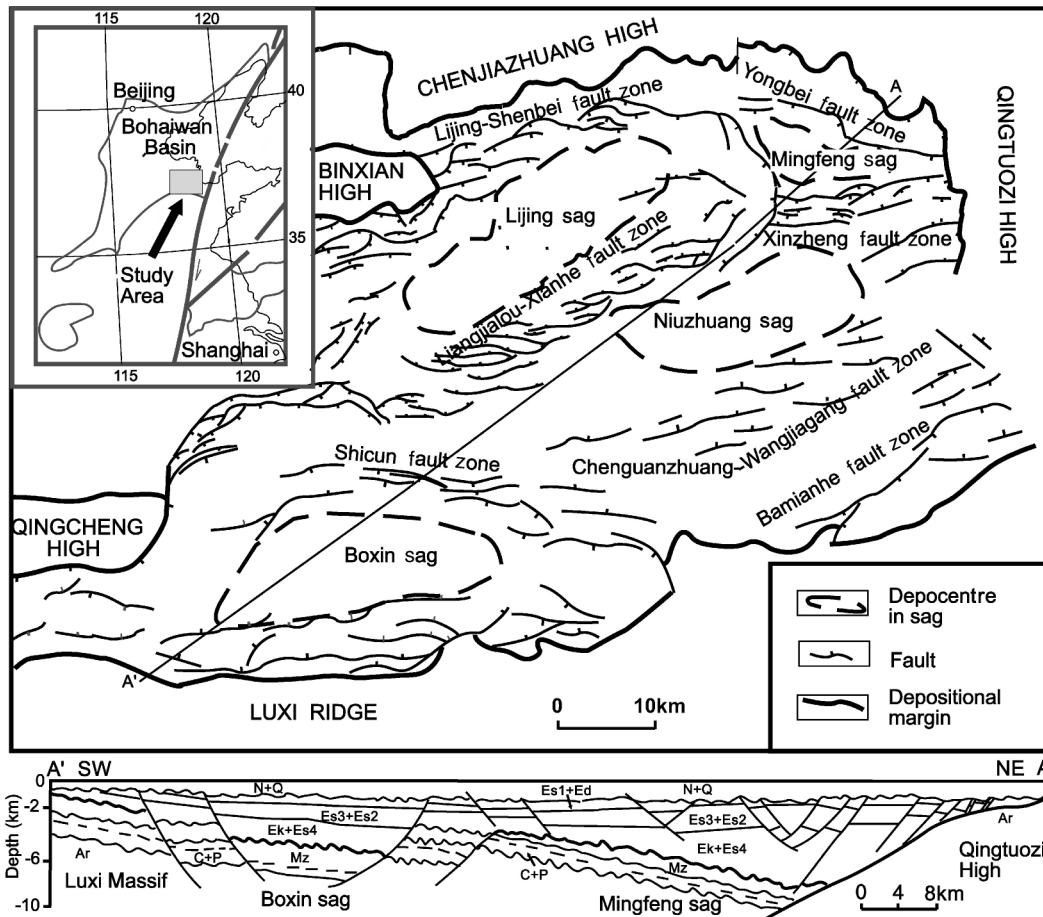
Fig. 1. Location map and cross-section (A–A′) showing the major structural features of the Dongying Depression in the Bohaiwan Basin, China.

The Dongying Depression located in the Bohaiwan Basin of China is a relatively young Tertiary basin that hosts a significant zone of strong overpressure. The origin of the overpressure in the Dongying Depression is, however, a subject of debate. The strongest overpressures (pressure gradients approaching $0.018\,\mathrm{MPa\,m^{-1}}$) are found near the depression's depocentres, where sedimentation has been most rapid. These areas, however, are also where hydrocarbon generation is most active.

In this paper, pressures measured during drill stem tests (DST) and calculated from well logs were used to document the distribution of overpressure in the Dongying Depression, and to explore the likely causes of this phenomenon. A numerical model of groundwater flow was then used to quantitatively examine the relationship between sediment compaction, hydrocarbon generation and the development of overpressure in the basin. The ultimate goal was to more accurately predict the location and magnitude of overpressures in this basin to allow more effective and safer exploitation of this resource.

GEOLOGICAL SETTING AND EXPLORATION HISTORY

The Dongying Depression, a northeast–southwest-trending sub-basin in the southern part of the Bohaiwan Basin, formed as a result of Tertiary rifting (Fig. 1). The sub-basin is bounded by the Luxi Massif in the south, the Qingtuozi High in the east, the Chenjiazhuang High in the north and the Qingcheng High in the west. The Dongying Depression is 60–100 km long, 40–65 km wide and covers an area of $5700\,\mathrm{km^2}$.

The depression has been explored for about 40 years and comprises one of the most prolific oil-producing provinces in the Bohaiwan Basin of China. The depression has attracted considerable attention because of the high quality of its source rocks and its considerable hydrocarbon potential (Kong *et al.* 1996; Li 1981; Xin *et al.* 1992; Zhou 1981). More than 30 oil pools have been discovered and more than 2000 exploration and development wells have been drilled to date. Most of the exploited traps occur in closed domes or faulted anticlines within the strata overlying the overpres-

sured sediments. Exploration in the past decade has focused on locating stratigraphic traps deeper in the basin, leading to the discovery of new oil pools within overpressured strata. These reservoirs occur in isolated lenses of sandstone, such as the turbidites of the Liangjialou oil field in the central basin, encased within the overpressured source rocks. The sandstones exhibit anomalously high pressures, comparable to those in the surrounding source rocks.

The structure of the Dongying Depression reflects the extensional tectonics of the region during the Tertiary (Li 1981). The interpretation of geological data and gravity profiles shows that a series of wedge-shaped rifts developed around the Bohai mantle rise as a result of crustal extension (Li 1981). Zhang & Tanimoto (1989) used tomographic inversion to verify the existence of the mantle rise. A recent study (Li et al. 1999) concludes that the evolution of the Bohaiwan Basin was controlled by both the mantle rise and dextral movement along the Tanlu pull-apart fault.

The Dongying Depression is bounded by the Lijing-Shenbei and Yongbei fault zones to the north, and by a mono-cline on the opposite side, forming a wedge-shaped basin. Seismic sections show that, on the monocline side, the basin structure is complicated by a series of small-scale normal faults, such as the Liangjialou-Xianhe and Chenjiazhuang fault zones (Fig. 1). These faults developed in an en echelon pattern as a result of dextral movement along the Tanlu fault. As a result of differential subsidence, the depression was dissected into four sags (the Lijing, Niuzhuang, Mingfeng and Boxin sags) separated from each other by uplifts (Fig. 1).

Figure 2 shows a generalized stratigraphic column for the region. Sediments filled the basin from the Palaeocene to the present, accumulating a maximum thickness of 7000 m. The geological history of the basin can be divided into distinct syn-rift and post-rift stages. Rifting occurred from the Palaeocene to the Oligocene, in four episodes (Fig. 2). During the early rifting, including syn-rifting stages I and II, deposition in the sub-basin was controlled by faults extending east–west.

Two east–west-trending depocentres were located in the Lijing–Mingfeng sag and the Boxin sag. The Palaeocene
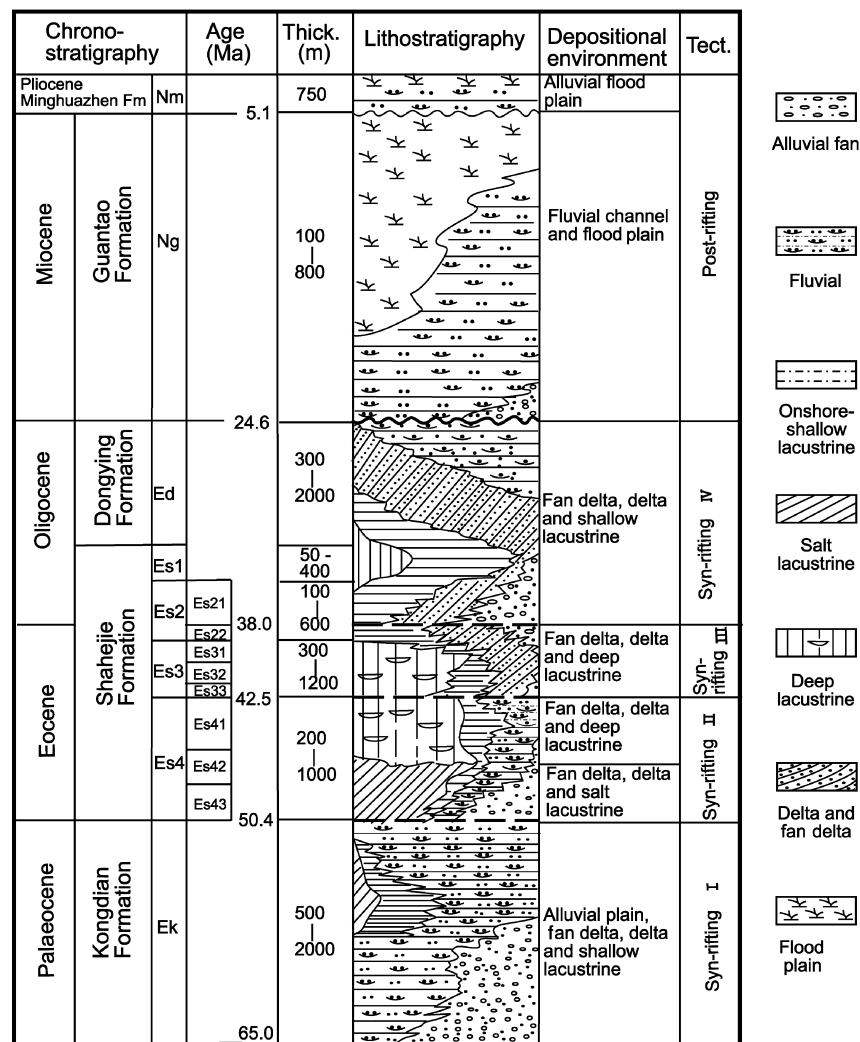

Fig. 2. Generalized geological column for the Dongying Depression.

Kongdian Formation, the lowermost unit, consists mainly of red siltstone, fine-grained sandstone and silty mudstone. The fourth member of the Shahejie Formation (Es4) includes two distinct parts. The upper submembers (including Es41 and Es42) are composed of shale and oil shale with a few sandstone beds, formed in deep lacustrine environments. These members contain mainly type I kerogen and comprise one of the several major source rocks for this basin. The lower interval (Es43) is composed mainly of interbedded lacustrine mudstone and gypsum and halite beds.

During late rifting, including syn-rifting stages III and IV, the direction of extension in the sub-basin changed from north–south to northwest–southeast, and the depocentres shifted to the Lijing sag. The third member of the Shahejie Formation (Es3) is composed of a coarsening-upward sequence. Thick lacustrine mudstones dominate the lower and middle parts, where isolated medium-grained sandstones with sharp upper and basal contacts are found; these units are considered to have been deposited by turbidity currents (Feng 1999). Shallow lacustrine deposits formed in the upper part before fan delta deposits covered the northern and north-western margins of the sub-basin. The Dongying delta developed along the eastern margin and spread westward, gradually prograding into the Niuzhuang and Lijing sags. As submember Es21 was deposited, small shallow lacustrine deposits and widespread delta plain deposits developed. During syn-rifting stage IV, interbeds of sandstones and mudstones formed in fan delta, delta and shallow lacustrine environments.

The post-rifting phase in the study area is represented by the Miocene Guantao and Pliocene Minghuazhen Formations. These units are composed of interbeds of medium-grained sandstones, siltstones and mudstones that formed in fluvial and flood plain environments.

METHODS OF STUDY

In this study, we evaluated the distribution of abnormal pressure in the basin by integrating direct pressure measurements from DST with pressures calculated from well logs. Direct pressure measurements were collected from nearly 1200 wells completed in reservoirs from the Palaeocene Kongdian to the Oligocene Dongying Formations. To determine the distribution of pressure in the fine-grained strata between reservoir rocks, we calculated the formation pressure from acoustic well logs. The calculated values allowed us to better determine the overall pressure distribution and to more precisely locate the top to overpressure.

Fluid pressure can be estimated from the sonic travel time because overpressured sediments tend to be undercompacted. As such, the profile of travel time versus depth in an overpressured basin commonly deviates from that in which compaction follows a normal trend with depth, as has been observed in a number of basins, such as in the Rocky Mountain region (Spencer 1987), the Laramide Basin
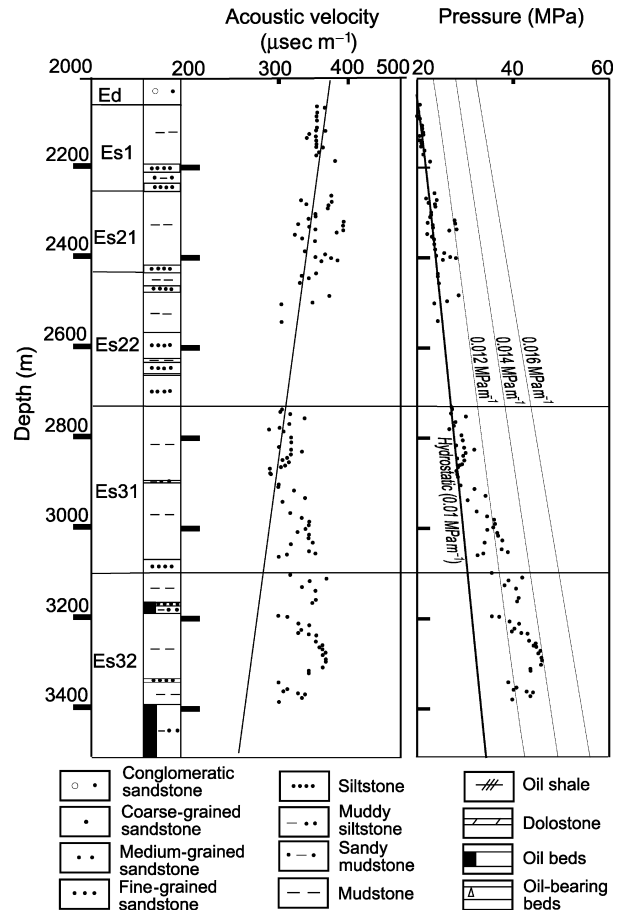

Fig. 3. Typical pressure versus depth profile for the Shahejie Formation, as calculated from an acoustic log. Profile is from well Shi119, the position of which is shown in Fig. 7. The method for calculating the pressure is described in the text.

(Surdam *et al.* 1997) and the central North Sea Basin (Osborne & Swarbrick 1997). In the overpressured sediments of the Dongying Depression, the departure of travel time from a normal trend line is clearly evident in acoustic well logs (Fig. 3).

We calculated the pressure within shales from log data using Magara's (1978) equation, which is based on the Terzaghi theory of shale compaction. In this method, the fluid pressure varies with the equivalent depth according to the relation

$$P_f = \rho_w g Z_E + \rho_s g (Z - Z_E) \qquad (1)$$

where P_f is the fluid pressure at a burial depth Z, Z_E the effective or equivalent depth, i.e. the depth at which the porosity expected along a normal compaction trend equals the actual porosity at depth Z, ρ_w the density of the formation water and ρ_s is the mean density of the sedimentary rocks. Z_E is given as

$$Z_E = -\frac{1}{C} \ln \frac{\Delta t}{\Delta t_o} \qquad (2)$$

where C is the compaction constant (m^{-1}), Δt is the transit time (sec) at depth Z_E within the normal compaction zone and Δt_o is the extrapolated surface transit time.

In compiling the pressure data, we used caliper logs to exclude values that might have been affected by poor hole conditions. We then categorized the data by lithology, according to the natural gamma log response. The primary effect of lithology, such as the different response of silty mudstones to siltstones, was therefore filtered out, but we made no attempt to further correct the data for any effects of mineralogy, such as the types of clay minerals present in a formation.

DISTRIBUTION OF ABNORMAL PRESSURES

Fluid pressure in reservoirs

We compiled reservoir pressure data from drill strata tests conducted in nearly 1200 wells in the study area. The majority of these data were taken from sandstone reservoirs in the

Eocene Shahejie Formation, which have been the main targets of hydrocarbon exploration in the basin.

As shown in Fig. 4, pressure gradients in the first and second members (Es1 and Es2) of the Shahejie Formation are mostly less than about 0.012 MPa m^{-1}. For comparison, a hydrostatic gradient is approximately 0.01 MPa m^{-1}. The third and fourth members (Es3 and Es4), however, are generally more highly overpressured, especially at depths below about 2200 m. At these depths, pressures considerably in excess of hydrostatic have developed with measured pressure gradients over the interval 2200–3000 m generally in the range $0.013–0.014 \text{ MPa m}^{-1}$ (Fig. 4), and up to 0.016 MPa m^{-1} in sediments below 3000 m.

Zhou (1981) reports an average geothermal gradient of $3.6 \,^{\circ}\text{C}$ per 100 m in the Dongying Depression, and an average surface temperature of $14.2 \,^{\circ}\text{C}$. These data can be
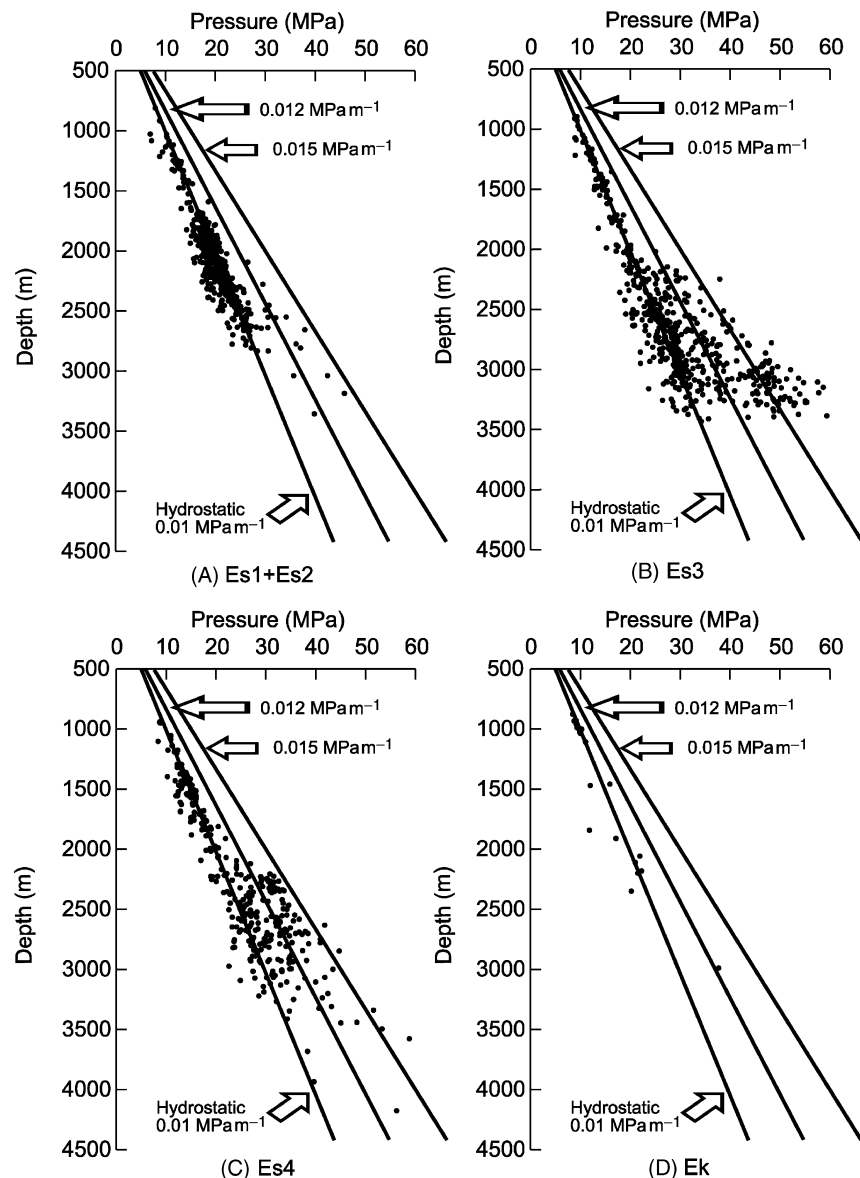

Fig. 4. Pressures measured in drill stem tests (DST) in different stratigraphic units: (A) members Es1 and Es2; (B) Es3; (C) Es4; (D) Ek. Strong overpressures can be seen below a depth of 2200 m within members Es3 and Es4 of the Shahejie Formation.

combined with past sedimentation rates to calculate the thermal maturity of source beds in the present day using the time-temperature index (TTI) method (Waples 1980). From these calculations, source rocks in the mature stage are expected at depths of 2200–3000 m, and highly mature source rocks from 3000 to 3800 m. The most overpressured reservoirs therefore occur in strata where petroleum is being actively produced in adjacent source beds. These reservoirs are located in sandstones that occur as isolated lenses within overpressured shales.

Fluid pressure in fine-grained lithologies

Fluid pressure versus depth plots in three wells located in the southern Lijing sag reveal three pressure systems within fine-grained lithologies (Figs. 3, 5, 6). The Oligocene and Miocene strata are normally pressured. A transitional interval occurs in submember Es31 where the pressure gradient rises from hydrostatic to about $0.013\,\text{MPa}\,\text{m}^{-1}$. Members Es32, Es33 and Es4 are overpressured. In general, the pressure gradient in submember Es32 is 0.001–$0.003\,\text{MPa}\,\text{m}^{-1}$ less

Fig. 6. Pressure–depth profile in the Shahejie Formation for well He139 (position shown in Fig. 7), showing the relationship between the abnormal pressure and lithology. Star shows pressure measured during a drill stem test. Legend for lithology is shown in Fig. 3.
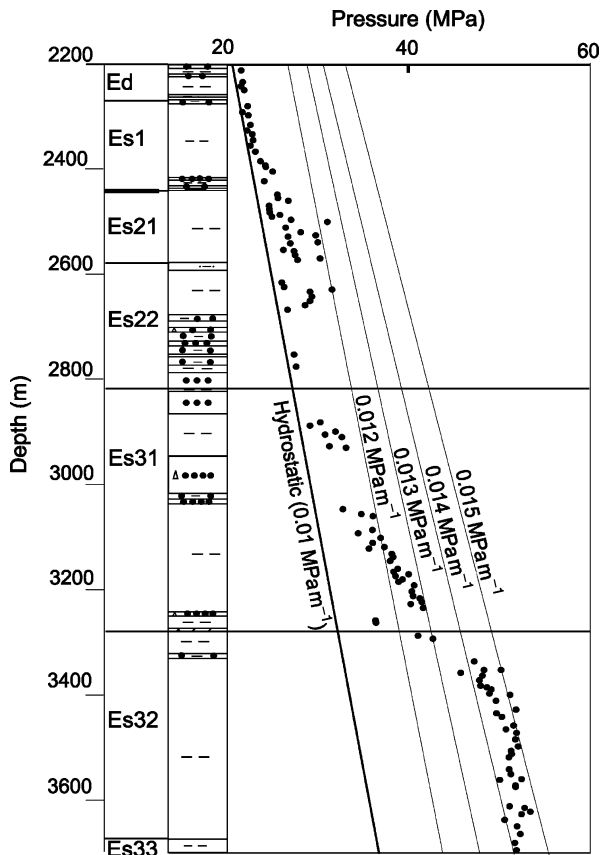

Fig. 5. Pressure–depth profile in the Shahejie Formation calculated from an acoustic log for well Li101 (position shown in Fig. 7), showing the relationship between the abnormal pressure and lithology. Legend for lithology is shown in Fig. 3.
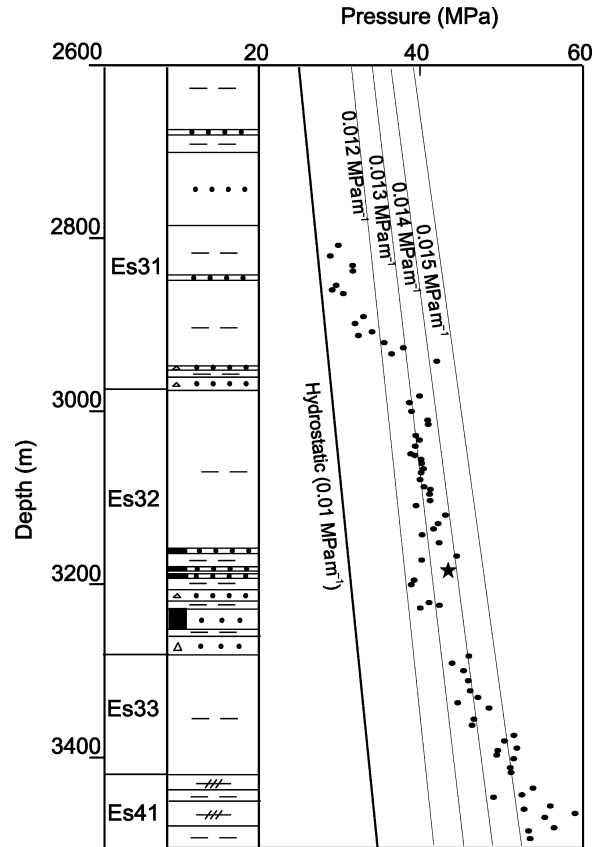
than that in Es33 and Es4. In Fig. 6, for example, pressure gradients in Es32 fall in the range 0.012–$0.014\,\text{MPa}\,\text{m}^{-1}$, whereas those in Es33 and Es4 increase to $0.018\,\text{MPa}\,\text{m}^{-1}$.

The pressure gradient near contacts between shale and sandstone, while considerably in excess of hydrostatic, is in many cases less than the gradient towards the centres of the shale layers, as shown in Figs 3 and 5. These sandstones are overpressured and, in many cases (for example, wells Shi119, Fig. 3, and He139, Fig. 6), oil-bearing. Shale beds here are apparently generating petroleum and supplying it directly to the sandstone reservoirs they contact.

Distribution of overpressure

To examine the distribution of overpressure in the Dongying Depression, we plotted two maps of the pressure coefficient (the ratio of the calculated to the hydrostatic pressure) along the top surfaces of submembers Es32 (Fig. 7) and Es33 (Fig. 8) using the pressure data calculated from well logs. Overpressured conditions (pressure coefficient > 1.2) are generally found near the centre of the sub-basin, especially
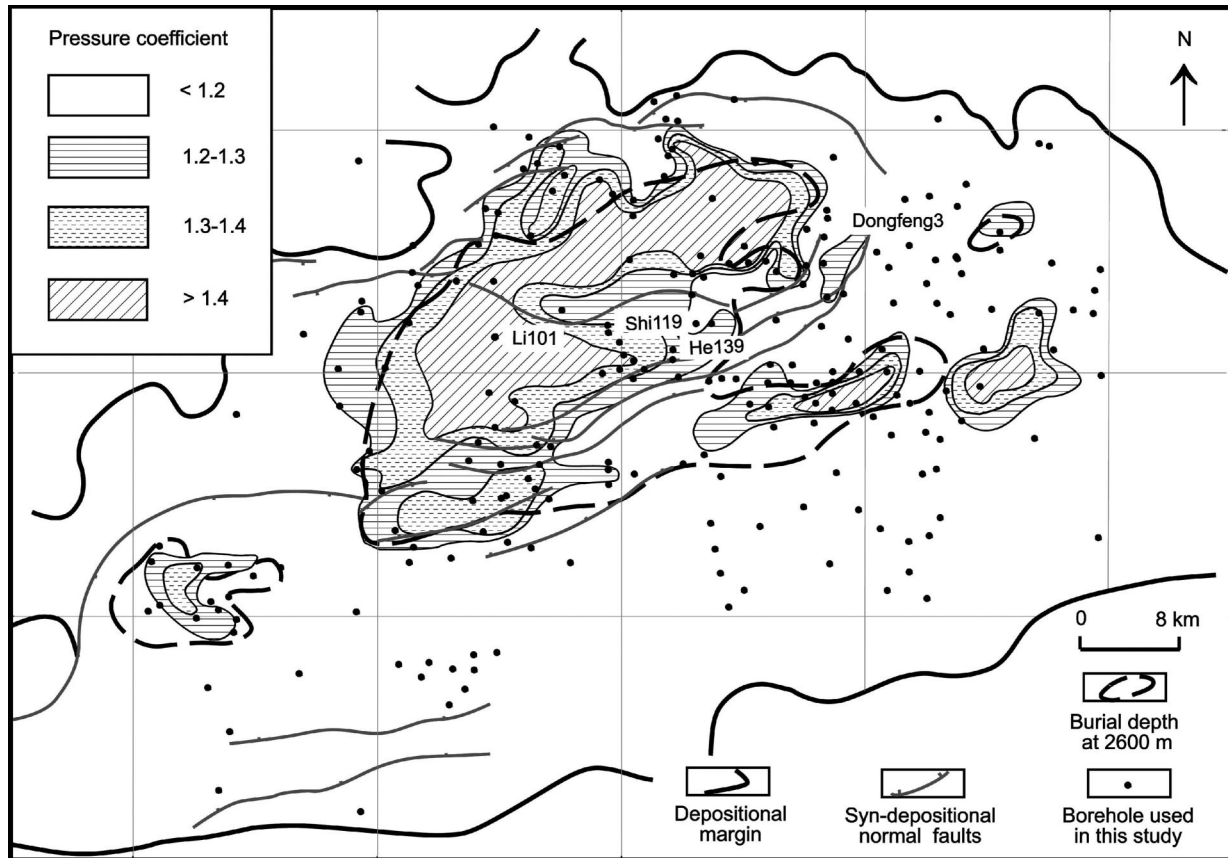
Fig. 7. Distribution of pressure gradient at the top of submember Es32. The zone of strong overpressure is coincident with the area where Es32 is buried below 2600 m. Also shown are the positions of the boreholes used in this study; those referred to in Figs 3, 5 and 6 are labelled.

around Lijing sag, along the depocentres of the late rifting stage. The zone of strong overpressure coincides roughly with the area where submember Es32 is buried in excess of 2600 m (Fig. 7). In Fig. 8, the area where the pressure coefficient exceeds 1.2 covers most of the Lijing and Niuzhuang sags. Strong overpressures (pressure coefficient > 1.4) are located where submember Es33 is buried to at least 3200 m. Hydrostatic and slightly overpressured conditions are found in the northern and eastern margins of the sub-basin.

On the basis of the data presented, we can draw the following conclusions about the distribution of overpressure in the Dongying Depression.

(1) Overpressure occurs mainly along the Lijing and Niuzhuang sags, where thick sequences of shale and oil shale, deposited in deep lacustrine environments, have become thermally mature.

(2) The magnitude of overpressure in submember Es32 is considerably less than that in Es33. Higher overpressures might have developed in Es33 because the submember has been more deeply buried than Es32, or because Es33

contains the oil-prone types I and II kerogen, whereas Es32 contains types II and III.

(3) Syndepositional faults in the central basin seem to have dissipated overpressure by allowing fluid to leak from deep strata. For example, approaching the Liangjialou-Xianhe fault zone, the pressure decreases sharply and the top of the overpressured system becomes deeper than in unfaulted strata. Figure 9 shows how the pressure decreases to nearly hydrostatic where the borehole encounters the fault. These fault zones probably not only focused fluid expulsion, but acted as conduits for hydrocarbon charge to fault-dependent traps. A large number of oil pays, such as the Shentuo field, the biggest oil field in the Dongying Depression, occur in normally pressured strata along the Liangjialou-Xianhe and Xinzheng fault zones.

(4) Conditions at the base of the overpressured zone are poorly known, because drilling in the central basin has seldom reached the Kongdian Formation. The few DST data available suggest that the pressure gradient in the Kongdian Formation is less than $0.013\,\mathrm{MPa\,m^{-1}}$ (Fig. 4). The relatively
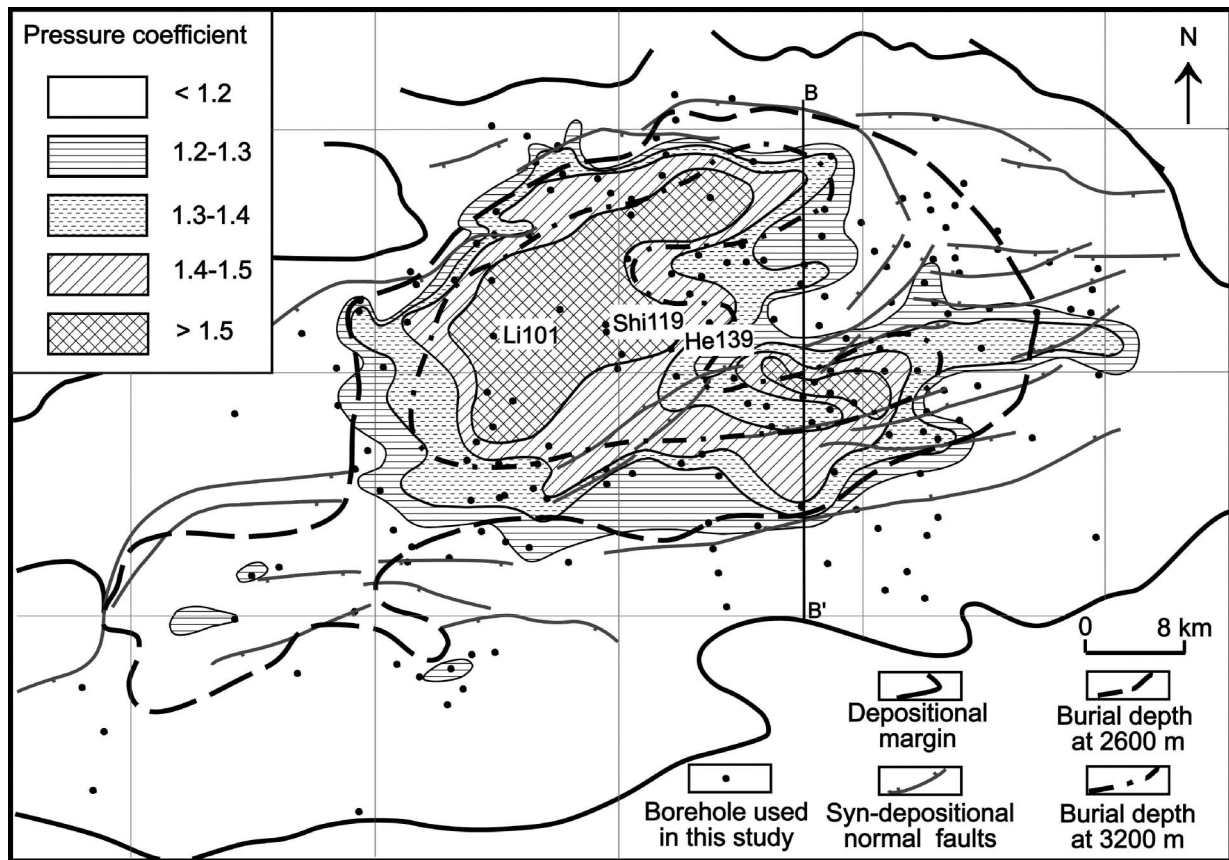
Fig. 8. Distribution of pressure gradient at the top of submember Es33. The zone of strong overpressure is coincident with the area where Es33 is buried below 3200 m. Also shown is the position of cross-section B–B′ referred to in Figs 10 and 13.

low pressure here may reflect in part the low organic content of the formation, where organic carbon averages 0.8%.

ORIGIN OF OVERPRESSURES

Many researchers have discussed possible causes of overpressures, including Fertl *et al.* (1994), Hunt (1990) and Law & Spencer (1998). Swarbrick & Osborne (1998) grouped the processes causing overpressure into three categories: stress-related (sediment compaction, lateral tectonic compression), fluid volume increase (thermal expansion, water release due to mineral transformation, hydrocarbon generation, cracking of oil to gas) and fluid movement and buoyancy (osmosis, hydraulic head transmitted from topographic highs, buoyancy due to density contrasts).

Each of these mechanisms can, in an appropriate situation, undoubtedly produce at least some excess fluid pressure. The question to be answered here is what mechanism or mechanisms dominate in the study area. The increases in fluid volume associated with thermal expansion and clay mineral dehydration are thought to be insufficient to generate significant overpressure, in the absence of a perfect hydraulic seal (Luo & Vasseur 1992; Osborne & Swarbrick 1997; Shi & Wang

1986). Lateral compression can cause overpressuring in accretionary prisms at plate margins, and in compressional basins, such as the Sacramento Basin (McPherson & Garven 1999). In the extensional tectonic environment of the Bohaiwan Basin, however, sediment compaction and hydrocarbon generation are the most likely of the proposed mechanisms to explain the generation of overpressure.

Effect of sediment loading on pressure development

In a sedimentary basin, disequilibrium compaction occurs when, due to rapid sedimentation, pore water cannot escape from the sediments at a rate sufficient to let them compact normally. In this case, the sediment remains undercompacted, and an unusually large share of the weight of the overlying sediment is borne by the pore fluid, leaving it overpressured. Overpressuring of this type is favoured where depositional rates are rapid, sediments compressible and permeability low (Bethke 1986; Burrus *et al.* 1996).

We used a numerical model of groundwater flow in sedimentary basins called Basin2 (Bethke 1985; Bethke *et al.* 2000), to simulate fluid flow and pressure development in the Dongying Depression. Our numerical model considers
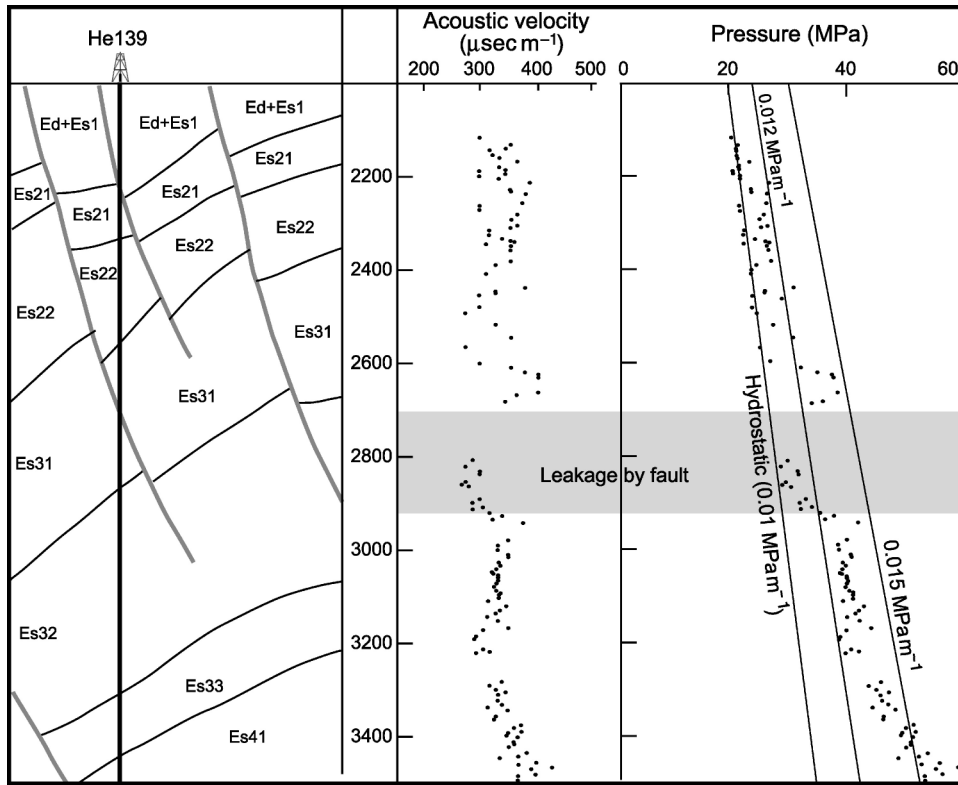
Fig. 9. Pressure profile for the Shahejie Formation showing the relationship between abnormal pressure and a fault cutting the borehole in well He139 (location shown in Fig. 7). Near-hydrostatic pressure is found in the shaded interval, between 2700 and 2900 m, but the surrounding strata are overpressured.

flow along a cross-section B–B′ (Fig. 8), which passes through the central part of the basin. To configure the model, we calculated stratigraphic thicknesses from seismic data. The structure of the section, which in the central basin is complicated by a number of postdepositional faults, was simplified considerably for the modelling. Specifically, we neglected the effects on stratigraphic thickness of small post-depositional faults. We assigned the fraction of sandstone in each stratigraphic unit in the model using data taken from wells along the section and adjacent to it. Table 1 lists the parameters used over the course of the simulation to calculate the porosity from the burial depth and fluid pressure, and the

permeability from the porosity. The latter calculation does not account explicitly for any effect of oil saturation on permeability.

Figure 10 shows the modelling results, which reflect the predicted effect of sediment compaction in generating overpressures, neglecting the effect of hydrocarbon generation. The results show that a zone of strong overpressure develops in members Es3 and Es4. Overpressure here exceeds 10 MPa, and the pressure gradient is larger than $0.0125 \, \text{MPa m}^{-1}$. Overpressuring in the model is greatest deep in the basin and decreases to hydrostatic towards the basin margin.

Table 1 Parameters used in the model to calculate porosity and permeability.

	Porosity*			Permeability†		
	ϕ_0	b (km^{-1})	ϕ_1	A	B	k_x/k_z
Sandstone	0.40	0.50	0.05	15	−5	2.5
Shale	0.55	0.85	0.05	8	−9	10
Evaporite	0.55	0.85	0.05	8	−8	10

*$\phi = \phi_0 \exp(-bZ_E) + \phi_1$, expressed as a fraction; Z_E is the effective burial depth (km).
†Log k_x (μm^2) = $A\phi + B$; $k_x \leq 1 \, \mu m^2$; $1 \, \mu m^2 \approx 1$ darcy.
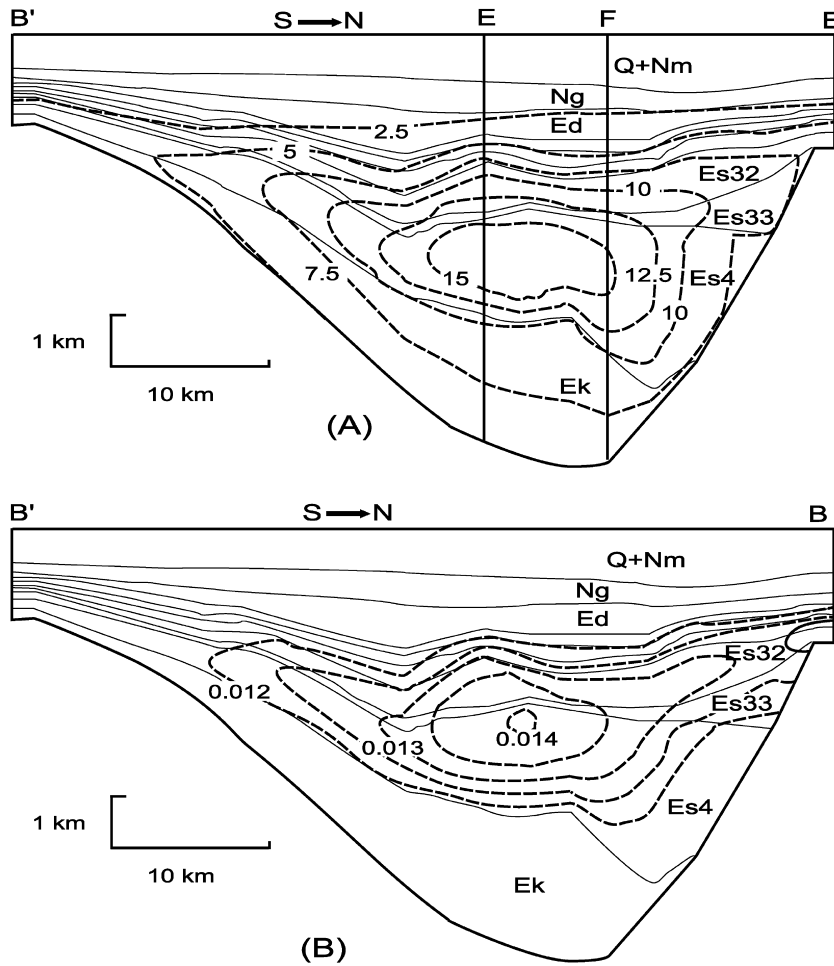
Fig. 10. Overpressure and pressure gradient along section B–B′ at the end of the simulation (present day), as calculated by the basin hydrology model. Model results show the overpressure that has arisen from sediment compaction, in the absence of the effects of hydrocarbon maturation. (A) Overpressure in MPa. (B) Pressure gradient in MPa m^{-1}. Fine lines separate stratigraphic units. Section extends about 52 km.

The sedimentation rate in the deep basin (Fig. 11) was relatively high during the deposition of Es4 and Es3, with rates of 200–450 m Ma^{-1}. Overlying strata, however, were deposited at a much slower rate, less than 100 m Ma^{-1}, except for the Pliocene Minghuazhen Formation, which accumulated at about 180 m Ma^{-1}. The overpressuring observed in the model is in part a remnant of rapid deposition at 65–40 Ma which has been preserved during a long interval of much slower deposition, from 40 to 5 Ma.

Effect of oil generation on pressure development

The conversion of solid kerogen to oil results in an increase in fluid volume and pressure, because the original kerogen is denser than the oil generated (Bredehoeft *et al.* 1994; Burrus *et al.* 1996; Lee & Williams 2000; Sweeney *et al.* 1995). As already mentioned, the primary overpressured strata in the Dongying Depression, the third and fourth members (Es3 and Es4) of the Shahejie Formation, are also the main source rocks. According to the data from the Shenli Oil
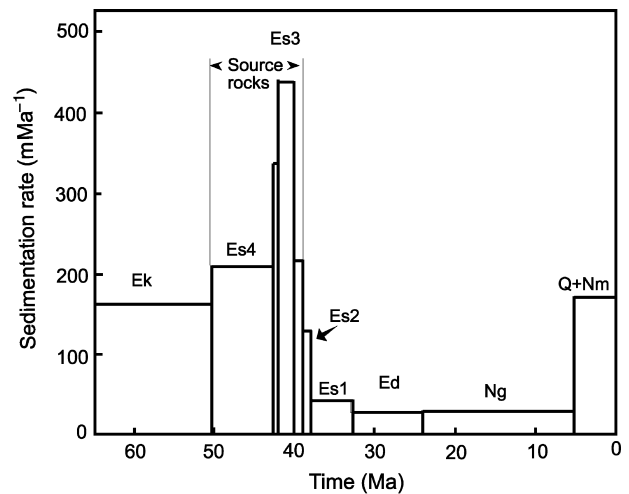

Fig. 11. Sedimentation rates (uncorrected for compaction) at location E in Fig. 10, about 30 km from the left of cross-section B–B′.

Table 2 Stratigraphic data used in the model.

Stratigraphic unit	Age (Ma)	Sand (%)	Source beds	TOC (%)	Kerogen
Quaternary and Pliocene (Q and Nm)	5.1	50			
Miocene, Guantao Fm. (Ng)	24.6	38			
Oligocene, Dongying Fm. (Ed)	32.8	38			
Oligocene, first members of Shahejie Fm. (Es1)	38	38–60	Shale	1.0	Type III
Oligocene, second members of Shahejie Fm. (Es2)	39	38–60	Shale	1.0	Type III
Eocene, upper third member of Shahejie Fm. (Es31)	40	25–30	Shale	1.5	Type III
Eocene, middle third member of Shahejie Fm. (Es32)	42	10–25	Shale	4.3	Types III and II
Eocene, lower third member of Shahejie Fm. (Es33)	42.4	5–15	Dark shale beds	5.5	Types II and I
Eocene, fourth member of Shahejie Fm. (Es4)	50.4	5–15	Oil shale, dark shale beds	9.6	Type I
Palaeocene, Kongdian Fm. (Ek)	65	20–38		0.8	Type III

TOC, total organic carbon.

Corporation, source beds of Es4 contain mainly type I kerogen (Zhou 1981) and have an average total organic carbon (TOC) of 2.4%. The source potential in Es3 varies vertically. Type II kerogen dominates the deeper layers, whereas mostly type III kerogen is found higher in the member. TOC decreases upwards, from average values of 2.2% in the lower submember of Es3 to 1.2% in the upper submember.

Most of the TOC data for Es33 and Es4 were collected from wells along the basin margin. In the central basin, however, TOC is higher than along the basin margin. Zhou (1981) argued that the average TOC of Es3 in the central basin, the area of greatest overpressuring, is more than 2% (Fig. 12). The highest organic carbon is present in submember Es33 and member Es4. For example, TOC reaches 7.3% at 3066 m in the Dongfeng 3 well.

These measurements represent the residual organic content after a fraction of the organic matter has been transformed to oil. Observation and laboratory results indicate that the various types of kerogen convert organic matter at

Fig. 12. Isolines of residual organic carbon in Es3, the third member of the Shahejie Formation (after Zhou 1981).

different efficiencies. Typical efficiencies X_o of converting organic carbon from types I, II and III kerogen are 0.895, 0.695 and 0.313, respectively (Tissot & Welte 1984). For example, the Green River Shale contains type I kerogen, and X_o is in the range 0.8–0.9. In other words, 80–90% of organic matter can be converted to oil. The Toarcian Shales of western Europe contain mostly type II kerogen, and X_o is 0.6. In our calculations, we assume X_o values for types I, II and III kerogen of 0.80, 0.60 and 0.20, respectively. Table 2 lists the values assumed for the original organic carbon content of each stratigraphic unit.

The rate of oil generation from a given kerogen at a given temperature can be calculated from an activation energy E_A and pre-exponential factor A_o, according to the Arrhenius equation. Because there has been no direct experimental determination of kinetic parameters for kerogen from the Dongying Depression, we used data for kerogen from other basins. Measured values (Issler & Snowdon 1990; Miknis & Turner 1988) of E_A and A_o for type I kerogen from the Green River Shale are $269\,kJ\,mol^{-1}$ and $8.54 \times 10^{20}\,h^{-1}$; for type II kerogen from the Woodford Shale of Oklahoma are $218.3\,kJ\,mol^{-1}$ and $6.51 \times 10^{16}\,h^{-1}$; and for type III kerogen from the Tent Island Shale of Canada are $230\,kJ\,mol^{-1}$ and $4.54 \times 10^{17}\,h^{-1}$.

To examine the relationship between oil generation and overpressure, we developed a model to simulate the evolution of overpressure associated with oil generation as well as sediment compaction. The modelling results show that overpressures of more than 10 MPa developed. The predicted pressure gradient in members Es32, Es33 and Es4 is larger than $0.0125\,MPa\,m^{-1}$, and reaches a maximum value of about $0.016\,MPa\,m^{-1}$ (Fig. 13). The predicted timing of hydrocarbon generation in Es4 source beds extends from the end of the Eocene to the present; generation in submembers Es33 and Es32 began in the Quaternary.

Comparing Figs 10 and 13, it is clear that organic maturation contributes to overpressuring within the source rocks, especially in Es33 and Es4. Figure 14 shows the contribution of thermal maturation to overpressuring, which ranges as
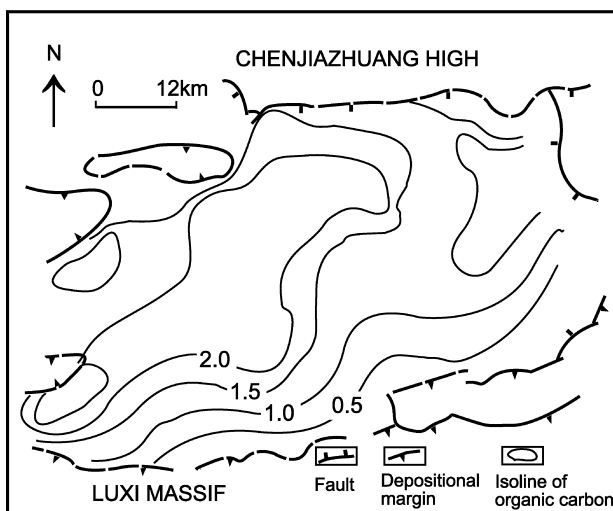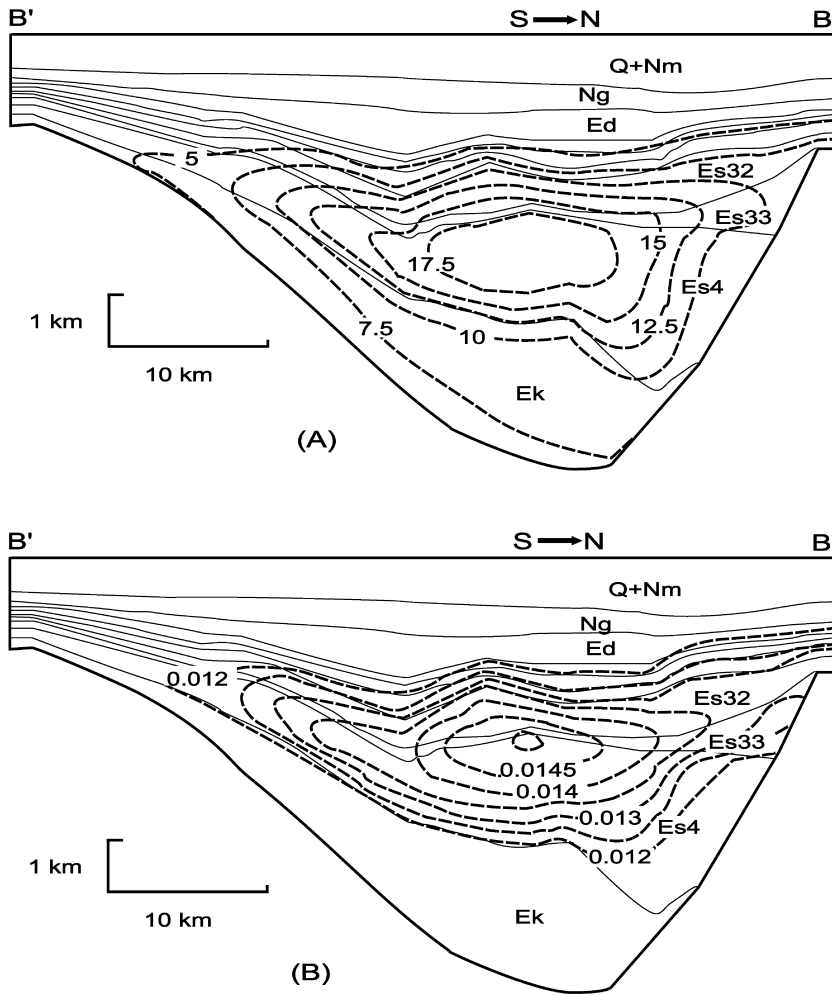
Fig. 13. Calculated overpressure and pressure gradient along section B–B′ in a simulation accounting for the effects of both sediment compaction and hydrocarbon maturation. (A) Overpressure in MPa; (B) pressure gradient in MPa m^{-1}.
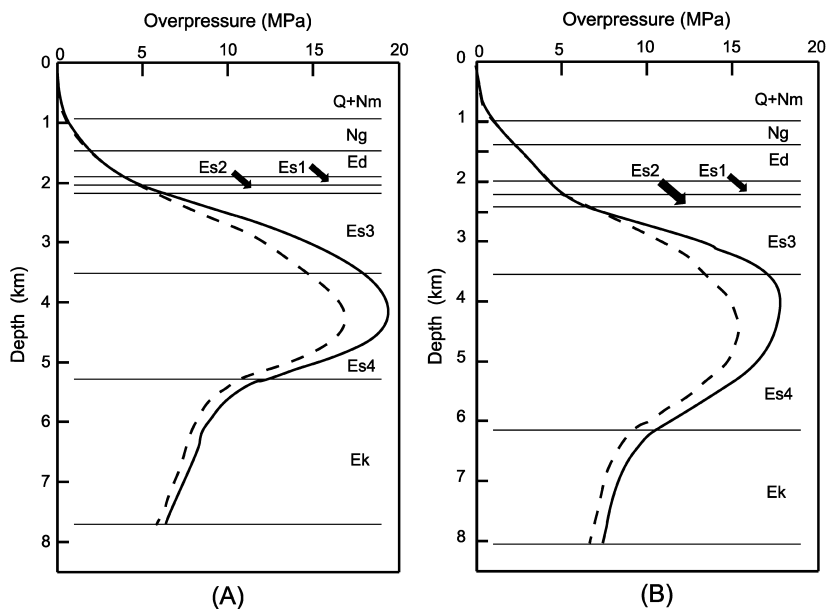

Fig. 14. Predicted overpressure profiles for locations E (A) and F (B) in Fig. 10. The broken line shows the overpressure predicted by a simulation accounting for compaction alone, and the full line shows the results when the effects of hydrocarbon maturation are included in the model.
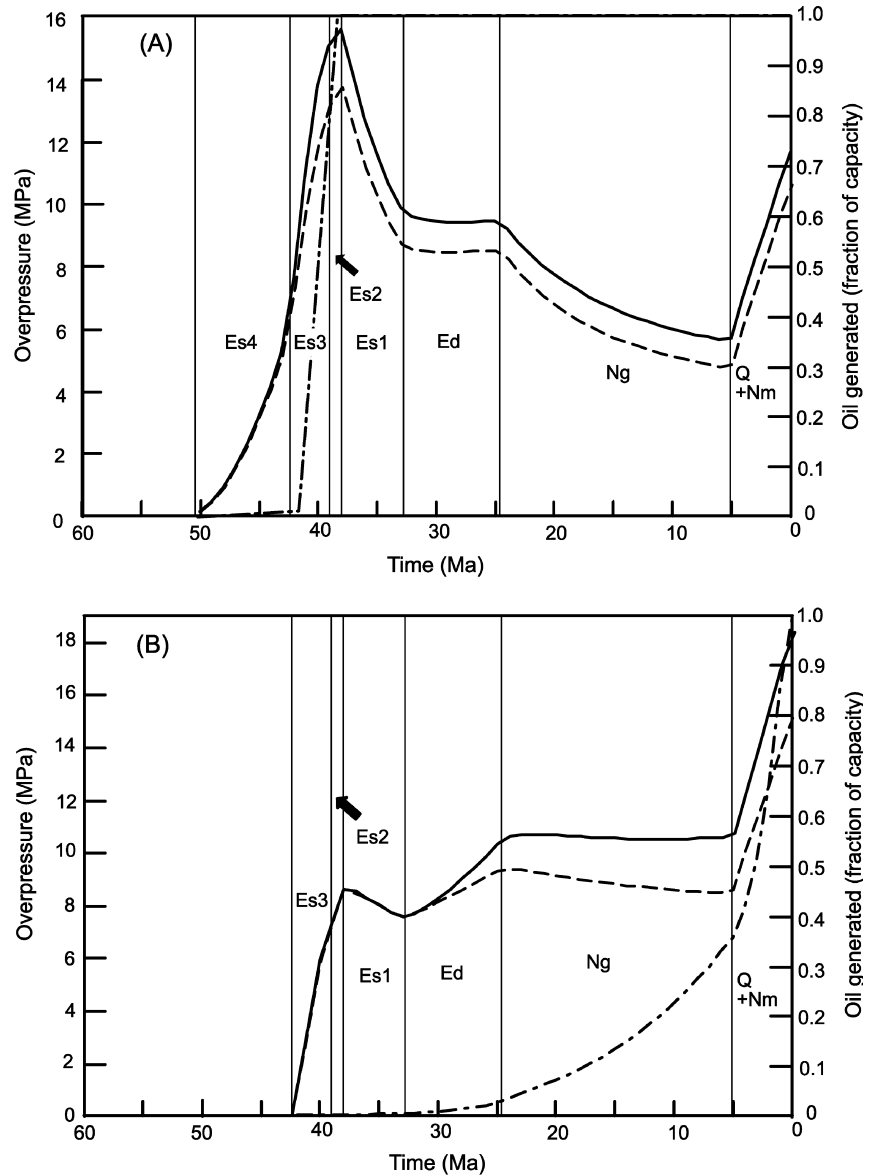
Fig. 15. Predicted evolution with time of overpressure and oil generation at the base of member Es4 (A) and submember Es33 (B) of the Shahejie Formation, at location E in Fig. 10. The full line shows the overpressure predicted by the simulation accounting for hydrocarbon maturation and sediment compaction, and the broken line shows results from the simulation accounting for compaction alone. The other line shows the oil generated within these strata versus time, expressed as a fraction of capacity.

high as several MPa in Es33 and Es4. In all cases, the role of thermal maturation in generating overpressure is subordinate to the effect of sediment compaction during burial. The model does not predict significant overpressures within the Palaeocene Kongdian Formation (Fig. 13) because these rocks were deposited at a low sedimentation rate and contain little organic matter.

Figure 15 shows how overpressure in the simulation develops through time at location E (see Fig. 10) at two depths: the base of member Es4 (plot A) and submember Es33 (plot B). Overpressure development is strongly related to the variation in sedimentation rate through time, as shown in Fig. 11. Overpressure increases most strongly during two intervals of rapid sedimentation in the overlying strata:

during the Eocene deposition of member Es3, and again within the past 5 Ma as Pliocene and Quaternary strata were deposited. Overpressure declines or remains about constant during Oligocene and Miocene time, when sedimentation was less rapid. Figure 15 also shows the secondary effect of oil generation on overpressure, as represented by the deviation of the predicted curves from those calculated by neglecting the effect of organic maturation. Overpressure develops most rapidly by this effect during the intervals of rapid oil generation at the depth in question.

Previous studies have emphasized the role of cracking organic matter to form natural gas, because the volume increase resulting from this process is very large (Bredehoeft *et al.* 1994; Hedberg 1974; Spencer 1987). In the Dongying

Depression, the burial depth of some source rocks reaches 3000–4000 m, which places them in the highly mature stage. Cracking of kerogen and the conversion of oil to gas can be expected to continue with time and burial, perhaps leading in the future to a dominant role of organic maturation over compaction in generating overpressure.

OVERPRESSURE DISTRIBUTION AND HYDROCARBON ACCUMULATION

A better knowledge of the origins of overpressure in the basin may improve our ability to analyse the migration and accumulation of hydrocarbon, because overpressure is one of the main forces driving hydrocarbon migration. A large number of oil pools have been found in the Dongying Depression in the normally pressured Oligocene strata overlying the overpressured Eocene sediments. Most reservoirs are found in one of three types of structural trap. The first type is within rollover anticlines on the downthrown sides of faults. This type of trap, exemplified by the Yanjia Oil Pool within the Lijing-Shenbei fault zone, is found mainly along the basin's northern margin. The other important types of traps are anticlinal structures associated with salt diapirs, and those associated with faulted blocks.

Each of the faulted blocks in the basin is unique in terms of the formations that host reservoirs, the thicknesses of pay sands and the position of the oil–water contact. In most cases, these oil pools are found in normally pressured strata that appear to be connected by syndepositional normal faults to overpressured source rocks. The faults have apparently served as conduits for petroleum migration.

Recent exploration has confirmed that, in addition to oil accumulations in normally pressured sediments, a considerable amount of oil can be found in sandstone reservoirs within the overpressured section. The oil is reservoired along the Liangjialou-Xianhe and Chenguanzhuang-Wangjiagang fault zones in Eocene turbidites and slump deposits of the fan delta facies of submembers Es31 and Es32, and in the southern basin within the delta front facies of member Es4.

It is interesting to note that syndepositional faults arranged in an en echelon pattern on the monoclinal side of the basin control not only the distribution of deep lacustrine source rocks, but the distribution of turbidite facies (Feng 1999; Li *et al.* 1999). Seismic studies have revealed adjacent to these faults more than 20 subtle stratigraphic traps, in which sandstone reservoirs are found in turbidite and fan delta facies within the lowstand system tract. For example, reservoir rocks in turbidite facies within submembers Es32 and Es33 were deposited adjacent to the Liangjialou-Xianhe and Chenguanzhuang-Wangjiagang fault zones, and those in fan delta deposits within Es4 developed adjacent to the northern Lijing-Shenbei fault zone (Li *et al.* 1999). These reservoirs are not only surrounded by active source rocks, but are connected to the syndepositional faults. Most of these sand

bodies would be expected to fall in the overpressured system according to the pressure gradient observed at the top of submembers Es32 and Es33, as shown in Figs 7 and 8.

Based on an integrated analysis of the hydrocarbon system, these subtle stratigraphic traps are prime candidates for the accumulation of large quantities of oil produced by the basin's high quality source rocks (Li *et al.* 1999). Isolated sandstone reservoirs in the overpressured zone therefore may represent a productive target for future exploration in the basin. The integrated analysis, furthermore, may provide information useful for improving the safety of drilling operations as exploration proceeds further into the overpressured section.

CONCLUSIONS

The results of this study show that overpressure in the Dongying Depression of the Bohaiwan Basin is concentrated in the more deeply buried parts of the basin and occurs primarily in mudstones and oil shales of the third and fourth members (Es3 and Es4) of the Eocene Shahejie Formation. These members are rich in organic carbon and comprise the main source rocks in the basin. The strongest overpressure is found near the depression's Eocene depocentres in the Lijing and Niuzhuang sags.

The results of numerical modelling suggest that the main cause of abnormally high pressure is disequilibrium sediment loading and compaction during Eocene time and since the Pliocene. Hydrocarbon generation within source beds provides a pressure generating mechanism of secondary importance. The distribution of overpressure can be predicted by reconstructing sedimentation and organic maturation in the basin, and this information can be used to optimize exploration strategies and improve safety during drilling.

REFERENCES

Bethke CM (1985) A numerical model of compaction-driven groundwater flow and heat transfer and its application to the paleohydrology of intracratonic sedimentary basins. *Journal of Geophysical Research*, **90**, 6817–28.

Bethke CM (1986) Inverse hydrologic analysis of the distribution and origin of Gulf Coast-type geopressured zones. *Journal of Geophysical Research*, **91**, 6536–45.

Bethke CM, Lee MK, Park J (2000) *Basin Modeling with Basin2: a Guide to Using the Basin2 Software Package*. University of Illinois, Urbana-Champaign, IL.

Bredehoeft JD, Wesley JB, Fouch TD (1994) Simulation of the origin of fluid pressure, fracture generation, and the movement of fluids in the Uinta Basin, Utah. *AAPG Bulletin*, **78**, 1729–47.

Burrus JK, Osadetz KG, Wolf S, Doligez B, Visser K, Dearborn D (1996) A two-dimensional regional basin model of Williston basin hydrocarbon systems. *AAPG Bulletin*, **80**, 265–91.

Dickinson G (1953) Geological aspects of abnormal reservoir pressure in Gulf Coast Louisiana. *AAPG Bulletin*, **37**, 410–32.

Feng YL (1999) Lower Tertiary sequence stratigraphic framework and basin filling model in Dongying depression. *Earth Science*, **24**, 613–24(in Chinese).

Fertl WH, Chapman RE, Hotz RF (1994) Studies in abnormal pressures. *Developments in Petroleum Science*, **38**, 454.

Hedberg HD (1974) Relation of methane generation to under-compacted shales, shale diapirs and mud volcanics. *AAPG Bulletin*, **58**, 661–73.

Hubbert MK, Rubey WW (1959) Mechanics of fluid filled porous solids and its application to overthrust faulting, 1: role of fluid pressure in mechanics of overthrust faulting. *Geological Society of America Bulletin*, **70**, 115–66.

Hunt JM (1990) Generation and migration of petroleum from abnormally pressured fluid compartments. *AAPG Bulletin*, **74**, 1–12.

Issler RD, Snowdon LR (1990) Hydrocarbon generating kinetics and thermal modeling, Beaufort-Mackenzie basin. *Bulletin of Canadian Petroleum Geology*, **38**, 1–16.

Kong FX, Zheng HR, Duan ZB, Li XH (1996) Study on Tertiary sequences, the sedimentary systems and basin filling history of Dongying Depression, Shandong, China. *30th International Geological Congress*, **30**, 176.

Law BE, Spencer CW (1998) Abnormal pressures in hydrocarbon environments. In: *Abnormal Pressures in Hydrocarbon Environments, AAPG Memoir 70* (eds Law BE, Ulmishek GF, Slavin VI), pp. 1–11. American Association of Petroleum Geologists, Tulsa, OK.

Lee MK, Williams DD (2000) Paleohydrology of the Delaware Basin, western Texas: overpressure development, hydrocarbon migration, and ore genesis. *AAPG Bulletin*, **84**, 961–74.

Li DS (1981) Geological structure and hydrocarbon occurrence of the Bohai Gulf oil and gas Basin (China). In: *Petroleum Geology in China* (ed. Mason JF), pp. 180–92. Pennwell Publishing Co., Tulsa, OK.

Li ST, Xie XN, Lu YC, Ren JY, Wang H, Chen HH (1999) *Studies on Sedimentology, Structure and Hydrocarbon Accumulation in Tertiary Dongyting Depression*, Shenli Oilfield Corporation Research Report (in Chinese). Shenli Oilfield Corporation, Shandong.

Luo XR, Vasseur G (1992) Contributions of compaction and aquathermal pressuring to geopressure and the influence of environmental conditions. *AAPG Bulletin*, **76**, 1550–9.

Luo X, Vasseur G (1996) Geopressuring mechanism of organic matter cracking: numrical modeling. *AAPG Bulletin*, **80**, 856–74.

Magara K (1978) Compaction and fluid migration: practical petroleum geology. *Developments in Petroleum Science*, **9**, 296.

McPherson B, Garven G (1999) Hydrodynamics and overpressure mechanisms in the Sacramento basin, California. *American Journal of Science*, **299**, 429–66.

Miknis FP, Turner TF (1988) *Thermal Decomposition of Tipton Member, Green River Formation of Oil Shale from Wyoming*, Report by Western Research Institute, Laramide, to Department of Energy. Western Research Institute, Laramide, WY.

Osborne MJ, Swarbrick RE (1997) Mechanisms for generating overpressure in sedimentary basins: a reevaluation. *AAPG Bulletin*, **81**, 1023–41.

Shi YL, Wang CY (1986) Pore pressure generation in sedimentary basins: overloading versus aquathermal. *Journal of Geophysical Research*, **91**, 2153–62.

Spencer CW (1987) Hydrocarbon generation as a mechanism for overpressuring in Rocky-Mountain region. *AAPG Bulletin*, **71**, 368–88.

Surdam RC, Jiao ZS, Heasler HP (1997) Anomalously pressured gas compartments in Cretaceous Rocks of the Laramide Basins of Wyoming: a new class of hydrocarbon accumulation. In: *Seals, Traps, and the Petroleum System, AAPG Memoir 67* (ed. Surdam RC), pp. 199–222. American Association of Petroleum Geologists, Tulsa, OK.

Swarbrick RE, Osborne MJ (1998) Mechanisms that generate abnormal pressures: an overview. In: *Abnormal Pressures in Hydrocarbon Environments, AAPG Memoir 70* (eds Law BE, Ulmishek GF, Slavin VI), pp. 13–34. American Association of Petroleum Geologists, Tulsa, OK.

Sweeney JJ, Braun RL, Burnham AK, Talukdar S, Vallejos C (1995) Chemical kinetic model of hydrocarbon generation, expulsion, and destruction applied to the Maracaibo Basin, Venezuela. *AAPG Bulletin*, **79**, 1515–32.

Tissot BP, Welte DH (1984) *Petroleum Formation and Occurrence*, 2nd edn. Springer-Verlag, Berlin.

Waples DW (1980) Time and temperature in petroleum formation, application of Lopatin's method to petroleum exploration. *AAPG Bulletin*, **64**, 916–26.

Xie XN, Li ST, Dong WL, Zhang QM (1999) Overpressure development and hydrofracturing in the Yinggehai basin, South China Sea. *Journal of Petroleum Geology*, **22**, 437–54.

Xin QL, Liu ZR, Jin Q (1992) The principles of tectonic lithofacies analysis of hydrocarbon-bearing basins. In: *Progress in Geology of China*, pp. 245–7. Geological Publishing House, Beijing.

Zhang YS, Tanimoto T (1989) Three-dimensional modeling of upper mantle structure under the Pacific Ocean and surrounding area. *Geophysical Journal of the Royal Astronomical Society*, **98**, 255–69.

Zhou GJ (1981) Character of organic matter in source rocks of continental origin and its maturation and evolution. In: *Petroleum Geology in China* (ed. Mason JF), pp. 26–47. Pennwell Publishing Co., Tulsa, OK.